International Journal of Environmental Sciences
ISSN: 2229-7359
Vol. 11 No. 24s, 2025
https://theaspd.com/index.php

A CFD Study And Comparison Of Different Nanoparticles-Water Combinations Flow And Conjugate Heat Transfer Performance In A 3-D Rectangular Duct

Ranajit Midya[1*], Rajat Kabiraj[2] and Snehamoy Majumder[3]
[1*,2]Research Scholar, Department of Mechanical Engineering, Jadavpur University, Kolkata-700032, India.
[3]Professor, Department of Mechanical Engineering, Jadavpur University, Kolkata-700032, India.

***Corresponding Author:** Ranajit Midya
*E-mail: ranajitmidya123@gmail.com

Abstract:
In this study, a three-dimensional numerical investigation is performed to evaluate the conjugate heat transfer performance of nanoparticles–water mixtures in a rectangular duct under steady, laminar flow conditions. The working fluids include Al_2O_3–water, CuO–water, and TiO_2–water, treated as homogeneous single-phase media with effective thermophysical properties determined by nanoparticle concentration. A constant heat flux is applied to the heated duct walls, while no-slip conditions are imposed at all fluid–solid boundaries. The governing equations for continuity, momentum, and energy are solved using a finite-volume based CFD approach to obtain detailed hydrodynamic and thermal characteristics. The analysis emphasizes the variation of velocity profiles, friction factor, overall heat transfer coefficient, and local Nusselt number. Simulations are conducted over a range of Reynolds numbers and nanoparticle volume fractions to capture the combined effects of flow intensity and particle loading. Results reveal that nanofluid suspensions significantly enhance convective heat transfer relative to the base fluid, with both the overall heat transfer coefficient and Nusselt number increasing with nanoparticle concentration. Higher Reynolds numbers further strengthen convective transport, confirming the synergistic role of inertia and nanoparticle dispersion. Among the nanofluids studied, Al_2O_3–water demonstrates the most balanced thermal enhancement, while CuO–water and TiO_2–water show comparatively lower but still notable improvements. The computational predictions were validated against available velocity data, ensuring model reliability. Overall, the comparative analysis confirms that nanoparticle–water mixtures can substantially enhance heat transfer in confined ducts, although optimization between thermal benefits and hydrodynamic penalties is essential. The findings provide valuable insight into nanofluid selection for advanced thermal system design.
Keywords: *Conjugative heat transfer, Nanofluids, Particle volume fraction, Nusselt number, Reynolds number.*

INTRODUCTION:

The study of nanofluid heat transfer has seen significant advancements over the past few decades, driven by the demand for enhanced thermal performance in compact heat exchange systems. Nanofluids are now widely explored in applications such as cooling of microelectronic devices, automotive radiators, and solar thermal collectors, where their superior thermal conductivity and convective heat transfer properties help achieve higher efficiency. The concept of nanofluids was pioneered by Choi and Eastman [1], who first demonstrated that dispersing nanoparticles in conventional fluids significantly enhances thermal conductivity. This foundational work provided the basis for subsequent research exploring convective heat transfer using nanofluids. Soon after, Xuan and Li [2] examined convective heat transfer enhancement and identified the influence of nanoparticle concentration and flow regime, emphasizing that nanofluids offer potential advantages for heat transport in practical applications.

To further quantify these effects, Akbarinia and Behzadmehr [3] conducted a numerical investigation of laminar mixed convection in horizontal curved tubes, showing that the addition of nanoparticles improved thermal performance. Recognizing the growing interest in this field, Wang and Mujumdar [4] provided one of the earliest comprehensive reviews, summarizing the experimental and numerical evidence on nanofluids and highlighting the challenges in stability and modeling. Complementary to this, Kakaç and Pramuanjaroenkij [5] presented a broader review of convective heat transfer in nanofluids, synthesizing results across geometries and flow regimes. The literature was further expanded by Malvandi and Galanis [6], who critically assessed how nanoparticle properties affect heat transfer, pointing to gaps in understanding related to particle-fluid interactions. Similarly, Vanaki et al. [7] produced a detailed review of numerical studies, categorizing progress in CFD modeling and comparing single-phase and two-phase approaches. These reviews collectively illustrate the trajectory from early demonstrations to advanced simulation-based analysis.

In parallel, the numerical foundation for heat transfer modeling was strengthened by Patankar [8], whose finite volume methods remain a standard in CFD simulations of nanofluid flow. Building on such frameworks, Kirez et al. [9] analyzed laminar nanofluid convection in circular tubes, providing numerical validation of enhanced heat transfer rates. Similarly, Heris et al. [10] examined Al_2O_3–water nanofluid in triangular ducts and reported higher Nusselt numbers than the base fluid, confirming geometric effects on enhancement.

For enclosure-based applications, Bouhalleb and Abbassi [11] numerically investigated CuO–water nanofluids in rectangular enclosures, observing improved natural convection performance. To better capture particle–fluid interaction, Vasefi and Alizadeh [12] adopted a two-phase Euler–Lagrange method for CuO–water nanofluids across different geometries, offering a more accurate depiction of momentum and heat exchange between phases. Beyond steady flows, Elyasi and Ziaei-Rad [13] studied pulsating laminar nanofluid flows in rectangular channels, showing that oscillatory conditions can further enhance convective heat transfer. Sundar and Suresh [14] extended investigations to microchannels using conjugate analysis, highlighting the importance of wall conduction. Likewise, Jafari and Aminossadati [15] performed conjugate heat transfer analysis in circular pipes, revealing that combined wall–fluid effects must be considered in practical design.

In the developing flow region, Rabby et al. [16] numerically explored water-based nanofluids in rectangular channels, confirming enhancement but also noting increased pressure drop penalties. Kashani et al. [17] investigated Al_2O_3–water nanofluids in annuli under constant wall temperature, validating improvement in laminar forced convection. Mixed convection cases were studied by Irmawati and Mohammed [18], who demonstrated strong buoyancy–nanoparticle coupling in rectangular ducts. Attention has also been given to hybrid base fluids. Boukerma and Kadja [19] analyzed Al_2O_3 and CuO nanofluids in water–ethylene glycol mixtures, observing tunable heat transfer performance depending on the mixing ratio. Similarly, Khudheyer et al. [20] studied finned tube geometries with Al_2O_3–water nanofluids and found higher convective performance compared to water alone, particularly beneficial in compact heat exchanger applications.

For alternative nanoparticles, Murshed et al. [21] experimentally investigated TiO_2–water nanofluids in laminar flow, reporting significant augmentation of convective heat transfer coefficients. Extending three-dimensional modeling, Bianco et al. [22] examined asymmetric heated channels and confirmed the consistent improvement of Al_2O_3–water nanofluids under laminar conditions. Barad and Makwana [23] numerically investigated microchannel cooling applications, finding that nanofluids improve both fluid flow and heat transfer, reinforcing their suitability for electronic cooling. The review by Omid et al. [24] provides a comprehensive discussion on entropy generation in nanofluid flows, emphasizing the influence of nanoparticle concentration, flow geometry, and boundary conditions on thermodynamic irreversibility. The study highlights that minimizing entropy generation is crucial for enhancing the energy efficiency of thermal systems using nanofluids.

Mathematical Formulation:

Problem Description:

Figure 1 illustrates the schematic representation of the physical model considered in this study. The nanofluid enters the duct with a uniform velocity U_{in}, and the flow is assumed to be steady and fully developed at the outlet, owing to a sufficiently long duct length relative to its hydraulic diameter. All duct walls are stationary, impermeable, and subject to the no-slip boundary condition. Thermal boundary conditions are applied such that a constant heat flux is imposed on the top and bottom walls, while the side walls are treated as adiabatic, ensuring no heat transfer occurs through them. The flow and heat transfer behavior are governed by the three-dimensional steady-state Navier–Stokes and energy equations in a Cartesian coordinate system, which are formulated as follows.

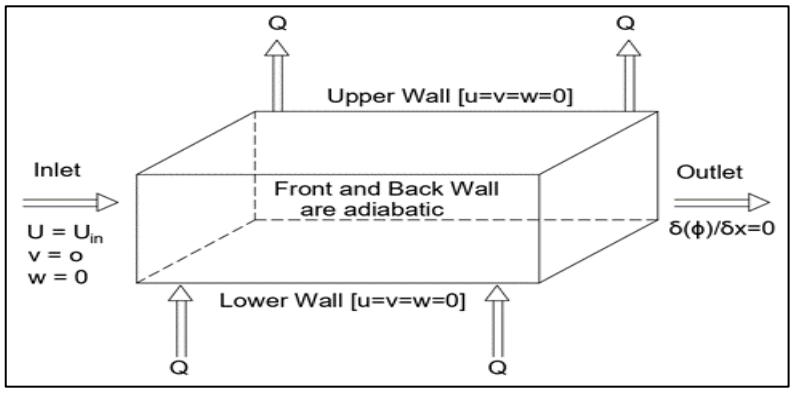

Fig. 1: The physical geometry and flow configuration of the horizontal rectangular duct

Governing Equations:
Continuity Equation:

$$\frac{\partial U}{\partial x}+\frac{\partial V}{\partial y}+\frac{\partial W}{\partial Z}=0 \quad [1]$$

X-Momentum Equation:

$$U\frac{\partial U}{\partial x}+V\frac{\partial U}{\partial y}+W\frac{\partial U}{\partial z}=-\frac{\rho_f}{\rho_{nf}}\frac{\partial P}{\partial x}+\frac{1}{R_e}\frac{\rho_f}{\rho_{nf}}\frac{\mu_{nf}}{\mu_f}\left[\frac{\partial^2 U}{\partial x^2}+\frac{\partial^2 U}{\partial y^2}+\frac{\partial^2 U}{\partial z^2}\right] \quad [2]$$

Y-Momentum Equation:

$$U\frac{\partial V}{\partial x}+V\frac{\partial V}{\partial y}+W\frac{\partial V}{\partial z}=-\frac{\rho_f}{\rho_{nf}}\frac{\partial P}{\partial y}+\frac{1}{R_e}\frac{\rho_f}{\rho_{nf}}\frac{\mu_{nf}}{\mu_f}\left[\frac{\partial^2 V}{\partial x^2}+\frac{\partial^2 V}{\partial y^2}+\frac{\partial^2 V}{\partial z^2}\right] \quad [3]$$

Z-Momentum Equation:

$$U\frac{\partial W}{\partial x}+V\frac{\partial W}{\partial y}+W\frac{\partial W}{\partial z}=-\frac{\rho_f}{\rho_{nf}}\frac{\partial P}{\partial z}+\frac{1}{R_e}\frac{\rho_f}{\rho_{nf}}\frac{\mu_{nf}}{\mu_f}\left[\frac{\partial^2 W}{\partial x^2}+\frac{\partial^2 W}{\partial y^2}+\frac{\partial^2 W}{\partial z^2}\right] \quad [4]$$

Energy Equation:

$$U\frac{\partial \theta}{\partial x}+V\frac{\partial \theta}{\partial y}+W\frac{\partial \theta}{\partial z}=\frac{\alpha_{nf}}{\alpha_f}\frac{1}{R_e.P_r}\left[\frac{\partial^2 \theta}{\partial x^2}+\frac{\partial^2 \theta}{\partial y^2}+\frac{\partial^2 \theta}{\partial z^2}\right] \quad [5]$$

Mathematical Modelling:
To investigate the heat transfer behaviors under laminar flow conditions, Al_2O_3–water nanofluids, CuO-water nanofluids and TiO_2-water nanofluids with varying nanoparticle volume concentrations—specifically 0%, 5%, and 10%—were utilized. The governing equations employed in this analysis are based on the formulations presented in reference [24].

The density of a nanofluid

$$\rho_{nf}=\varphi.\rho_s+(1-\varphi)\rho_w \quad [6]$$

Viscosity of the nanofluid

$$\mu_{nf}=\mu_w.(1+2.5\varphi) \quad [7]$$

The equation of specific heat of the nanofluid

$$C_{p_{nf}}=\frac{\varphi.\left(\rho_s.C_{p_s}\right)+(1-\varphi).\left(\rho_w.C_{p_w}\right)}{\rho_{nf}} \quad [8]$$

Effective thermal conductivity of the nanofluid:

$$k_{nf}=\left[\frac{k_s+2k_w+2(k_s-k_w)(1+\beta)^3\varphi}{k_s+2k_w-(k_s-k_w)(1+\beta)^3\varphi}\right]k_w \quad [9]$$

Convective heat transfer coefficient:

$$\overline{h_{nf}}=\frac{q}{A.(T_w-T_b)_{nf}} \quad [10]$$

Where, T_b is the bulk mean temperature at a cross section.
Nusselt Number of the nanofluid

$$\overline{Nu_{nf}}=\frac{\overline{h_{nf}}.D_h}{k_{nf}} \quad [11]$$

Friction factor is given by:

$$f=\frac{\mu_{nf}\frac{\partial U}{\partial y}}{0.5\rho_f {U_{in}}^2} \quad [12]$$

Boundary Conditions:

WALLS

$$U = V = W = 0,\ \dot{q} = -k\frac{\partial \theta}{\partial y} \quad [13]$$

INLET

$$U = U_{in},\ W = V = \theta = 0 \text{ (at the entrance, z=0)} \quad [14]$$

EXIT

$$\frac{\partial(\alpha)}{\partial x} = 0, \text{ (Fully developed condition),} \quad [15]$$

Where $\alpha = f(U, V, W, \theta)$ etc.

The dimensionless forms are interpreted as follows:

$$X = x / D_h;\ Y = y / D_h;\ Z = z / D_h;\ U = u / U_{in};\ V = v/U_{in};\ W = w/U_{in};\ \theta = (T-T_{in}) / (T_w - Tin), \quad [16]$$

$$P = \frac{p}{\rho_f U_{in}^{\ 2}},\ R_e = \frac{U_{in} D_h \rho_f}{\mu_f},\ P_r = \frac{\mu_f}{\rho_f \alpha_f} \quad [17]$$

SOLUTION METHODOLOGY:

A fully staggered grid system was used to solve the governing equations of fluid flow and heat transfer. In this approach, pressure and temperature are stored at the cell centres, while velocity components are positioned at the cell faces. Such an arrangement improves numerical stability and accuracy in incompressible laminar flows and prevents non-physical checkerboard patterns. The continuity, momentum, and energy equations were discretized through the finite volume method (FVM), ensuring strict conservation of mass, momentum, and energy within each control volume. The computational domain was divided into a structured mesh, and the fluxes across control surfaces were evaluated using the control volume approach.

For the discretization of convective terms, the power-law scheme of Patankar [8] was applied, offering a balance between stability and accuracy by combining upwind and central differencing. Pressure–velocity coupling was addressed with the SIMPLER (Semi-Implicit Method for Pressure-Linked Equations Revised) algorithm, which reduces pressure oscillations and enhances convergence compared to the SIMPLER method. Grid independence and validation studies confirmed the reliability of the adopted numerical methodology.

RESULTS AND DISCUSSION:

This study numerically investigates the hydrodynamic and thermal characteristics of nanofluid flow through a three-dimensional duct. Simulations were carried out for Reynolds numbers of 100, 500, 1000, and 2000 to assess the role of inertial forces on flow development and heat transfer. The influence of nanoparticle concentration was also examined by considering volume fractions of 0%, 5%, and 10%, thereby quantifying the enhancement in thermal performance with nanoparticle addition. Three nanofluid types Al_2O_3–water, CuO–water, and TiO_2–water was analyzed, with effective thermophysical properties estimated using mixture theory. The nanofluids were modeled as homogeneous, single-phase media under the assumptions of thermal equilibrium and no slip between nanoparticles and the base fluid. This formulation reduces complexity while maintaining accuracy for dilute to moderate nanoparticle loadings.

At the duct inlet, a uniform axial velocity and constant temperature were prescribed, representing an idealized plug-flow condition with a consistent thermal boundary. These boundary conditions provide a controlled framework to investigate the progressive development of velocity and thermal boundary layers along the duct length, enabling detailed evaluation of nanofluid behavior under laminar flow conditions.

Grid Independent Study and Validation:

Figure 2 shows the grid independence study for axial velocity profile at a representative cross-section. A comparison between different mesh densities confirms convergence of the solution, as evident from the negligible deviation between the velocity curves. To ensure the reliability and accuracy of the numerical model, a grid

independence study was conducted. Two different grid resolutions—101 × 15 × 15 and 201 × 15 × 15—were tested. As shown in Figure 2, the results obtained from both grids demonstrated excellent agreement, indicating minimal sensitivity to grid size. Consequently, the finer grid (201 × 15 × 15) was selected for all subsequent simulations to enhance solution accuracy and stability. The axial velocity profile exhibits a symmetric parabolic distribution, which is characteristic of fully developed laminar flow in a rectangular duct geometry. The overlap of both curves is nearly exact across the entire vertical domain. Minimal deviation is observed, especially near the peak velocity region (Centre of the channel), which is often the most sensitive to mesh refinement. The grid independence analysis was carried out for a representative case with Reynolds number Re=500 and nanoparticle volume fraction ϕ=1%, where a near-perfect overlap in results confirmed the robustness of the computational scheme.

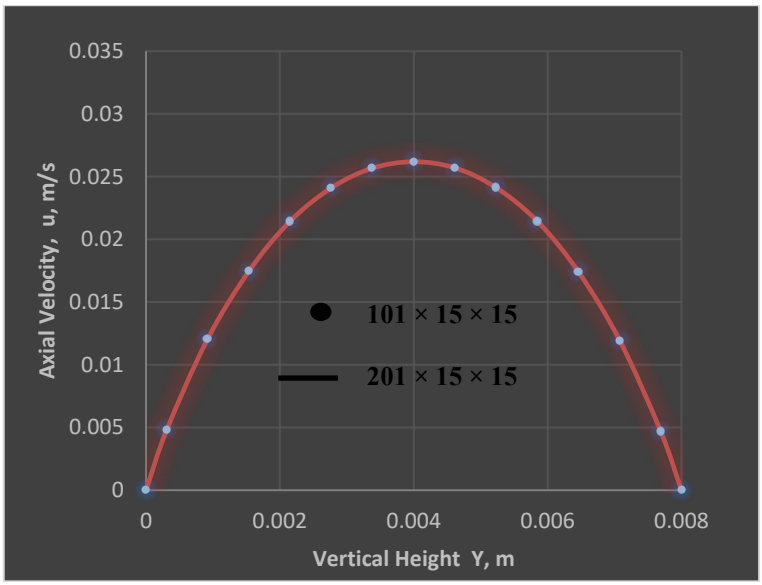

Fig. 2: The Grid Independent Study

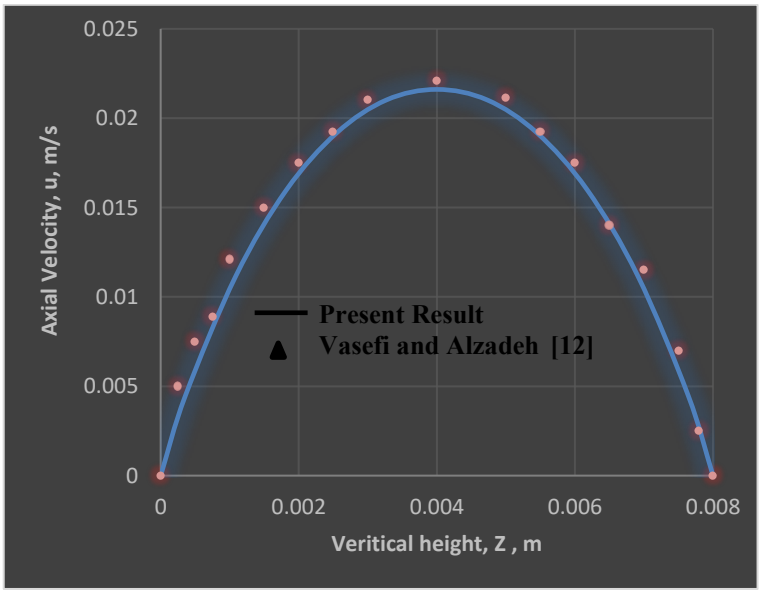

Fig. 3: Validation of Present Study

Figure 3 shows the validation of the axial velocity profile against published data by Vasefi and Alzadeh [12]. The strong agreement between the present simulation and the benchmark confirms the accuracy of the numerical model. The validation of the present result is carried out by comparing results of [12] shown in Figure 3. The figure presents a comparison of axial velocity (u) along the vertical height (Z) of the flow channel. The solid line represents the present numerical results. The triangular markers correspond to the benchmark data from Vasefi and Alzadeh [12], a peer-reviewed study. It is observed that the velocity profile exhibits a parabolic shape, which is consistent with laminar flow in a duct or parallel channel. There is an excellent agreement between the present results and the benchmark data across the entire channel height. The maximum deviation is minimal and likely

within numerical or experimental uncertainty bounds. This confirms that the numerical approach, boundary conditions, and discretization schemes are correctly implemented.

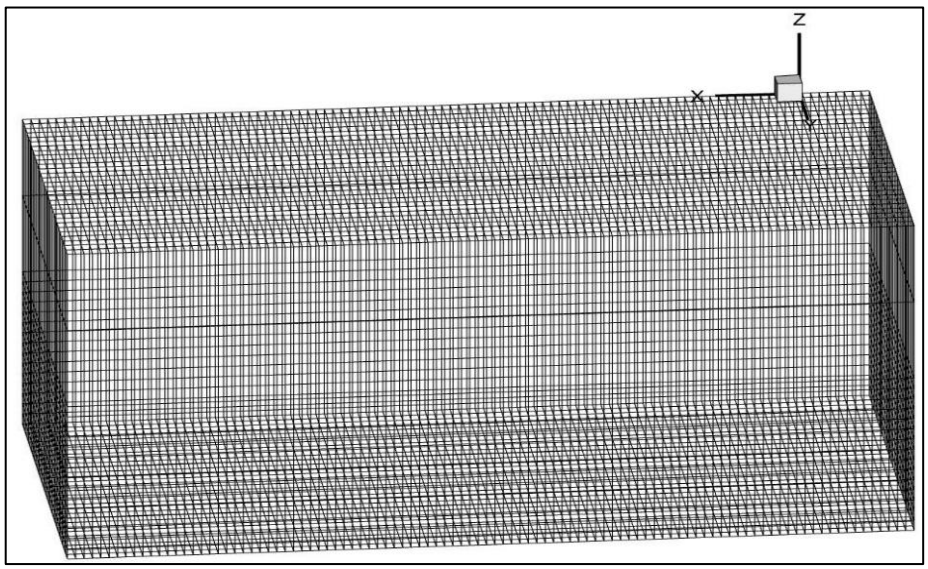

Fig. 4(a): Typical 3D Mess

In the figure 4(a), a 3-D geometry with the generated grids has been shown.

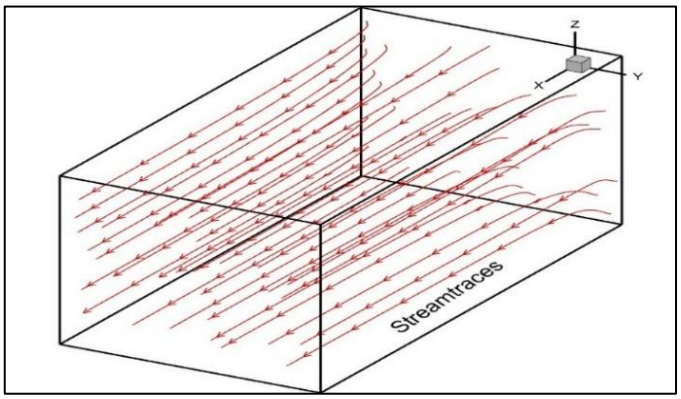

Fig.4(b): Stream traces

The figure 4(b) shown a 3-d geometry where stream traces have been shown. The diagram depicts that stream traces are parallel at the mid and exit planes, which is in accordance with the boundary conditions.

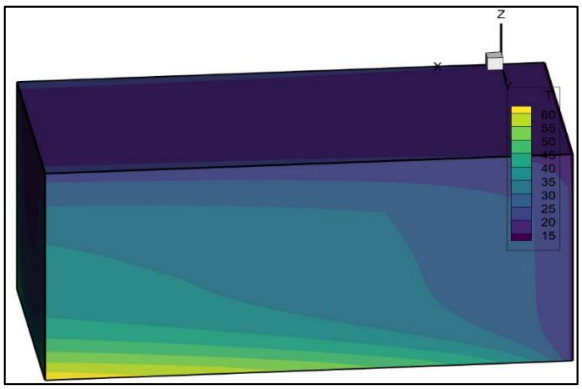

Fig.4(c): Temperature contour throughout the body.

The figure 4(c) shows the same 3-D figure with a contour of temperature and it amply explains the different heat transfer zones and temperature zones of the geometry while the conjugate heat transfer is going on.

International Journal of Environmental Sciences
ISSN: 2229-7359
Vol. 11 No. 24s, 2025
https://theaspd.com/index.php

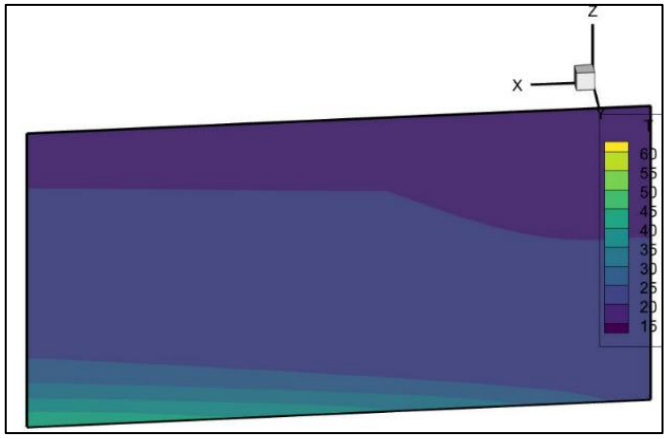

Fig4(d): Temperature contour in the mid plane

The above 4(d) diagram is a mid-longitudinal section of temperature contours in a 2-D configuration. It is shown to explain the heat transfer in the mid plane in an asymmetric temperature boundary condition. The figure shows that heat transfer is maximum near the wall. It should be mention that figures 4(b) to 4(d) pertaining to CuO nanofluid only.

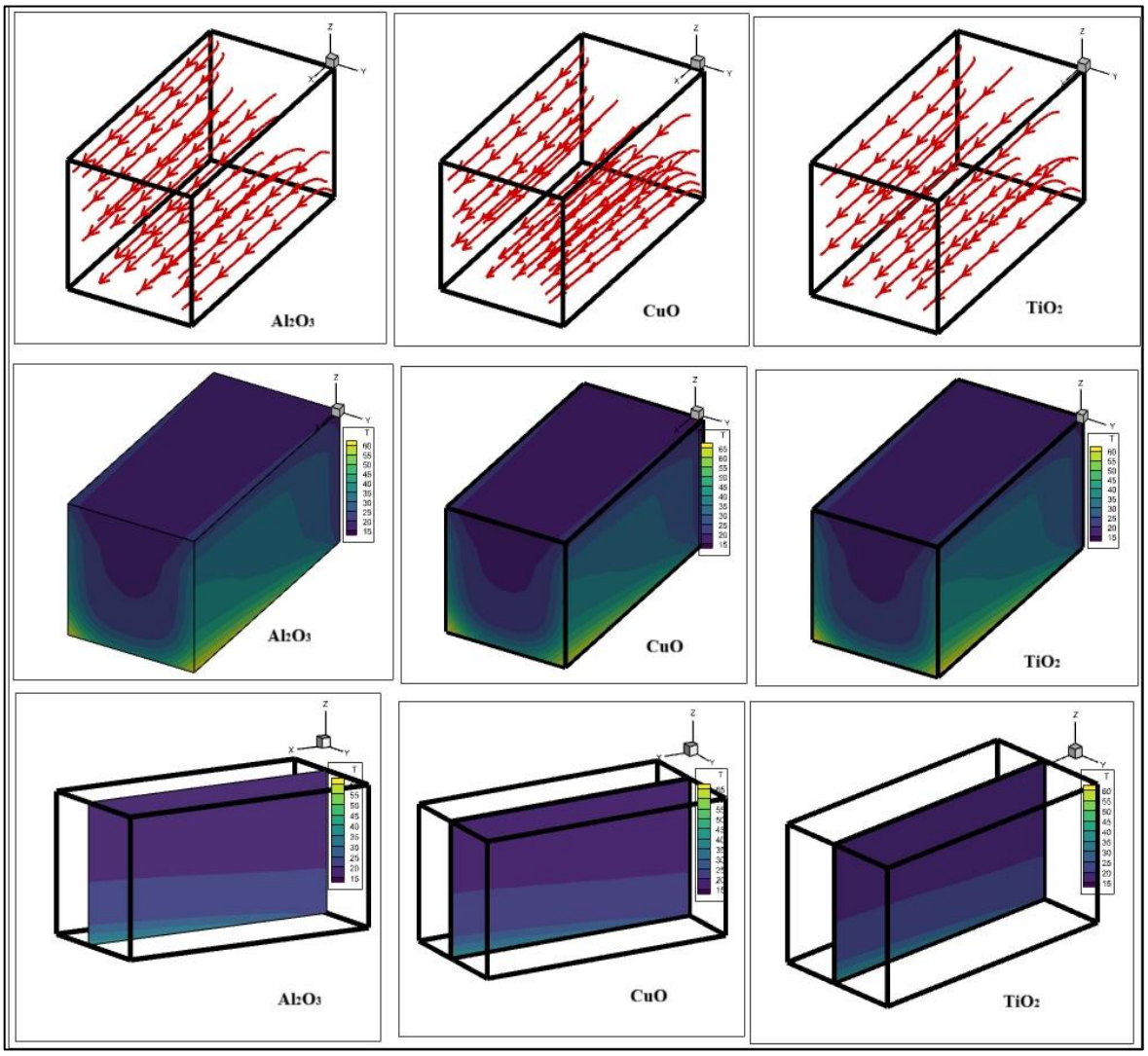

Fig.4(e): Stream Traces, Temperature contour throughout the body and the mid plane of Al_2O_3-water, CuO-water and TiO_2-water nanofluids.

Figure 4(e) presents the stream traces, temperature fields within the domain, and mid-plane contours for Al_2O_3–water, CuO–water, and TiO_2–water nanofluids under steady laminar conditions. The streamline plots (top row) show a nearly uniform velocity profile, confirming fully developed laminar flow. There are slight differences in

streamline density reflect variations in momentum diffusion caused by nanoparticle properties. The temperature contours (middle row) highlight the thermal boundary layer development along the heated walls. Al_2O_3–water displays the most uniform distribution across the duct, reflecting improved heat spreading compare to CuO–water and TiO_2–water nanofluids. The mid-plane temperature contours (bottom row) emphasize comparative performance. Overall, nanofluid type strongly affects flow and heat transfer. Al_2O_3–water provides the highest enhancement, CuO–water offers moderate improvement, and TiO_2-water shows relatively weaker performance.

Friction Factor Variation of different nanofluids:

The friction factors for all of the walls have been almost same values along the streamwise direction. The figures 5(a) and 5(b) represents friction factor variation at Reynolds number of 100 and 500 with particle volume concentration of 5%.

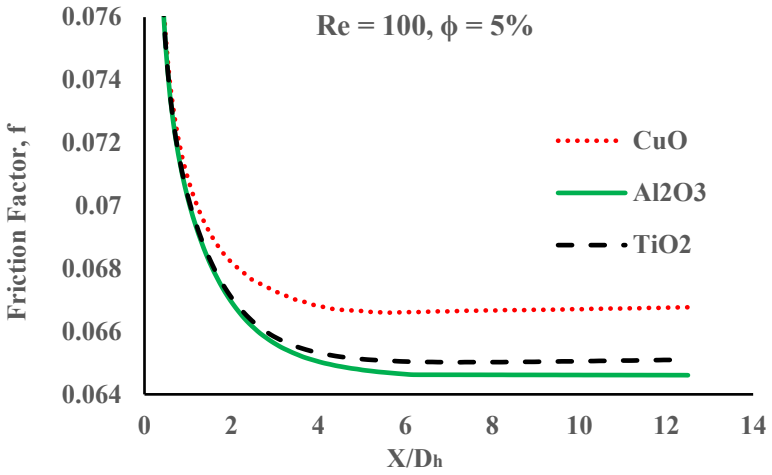

Fig. 5(a): Friction factor variations of different nanofluids at 5% volume concentration when Reynolds number is 100

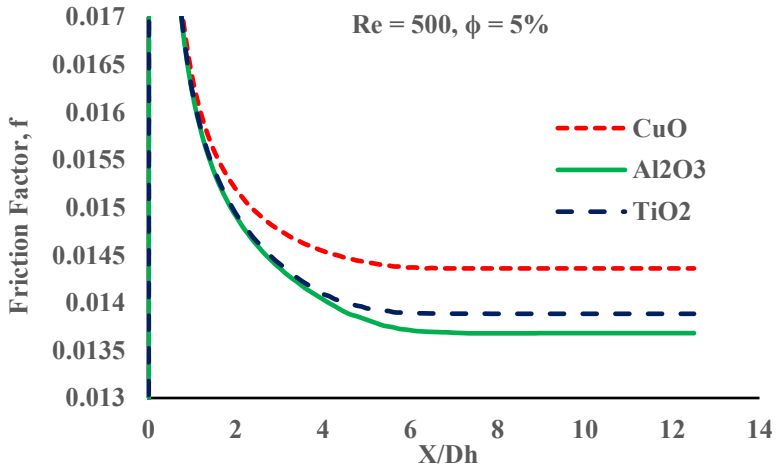

Fig. 5(b): Friction factor variations of different nanofluids at 5% volume concentration when Reynolds number is 500

Figures 5(a) and 5(b) illustrate the variation of the friction factor (f) along the dimensionless axial distance (X/D_h) for Al_2O_3–water, CuO–water, and TiO_2–water nanofluids at a fixed particle volume fraction of ϕ = 5% under Reynolds numbers of 100 and 500. At Re = 100 [Figure 5(a)], the friction factor decreases rapidly in the entrance region before reaching an almost constant value in the fully developed zone. CuO–water shows the highest values throughout the duct, followed by TiO_2–water, while Al_2O_3–water consistently yields the lowest. This behaviour is mainly linked to the higher viscosity and density of CuO nanoparticles, which enhance viscous drag, whereas Al_2O_3 offers lower flow resistance under laminar flow.

At Re = 500 [Figure 5(b)], the same decreasing trend is observed near the entrance, but the friction factors are notably lower than at Re = 100, confirming the inverse dependence of friction factor on Reynolds number. The differences among nanofluids become smaller at this higher Reynolds number due to the increasing influence of inertial effects. Overall, Al_2O_3–water emerges as the most hydrodynamically efficient nanofluid, while CuO–

water, although thermally advantageous, imposes greater frictional losses that require consideration in engineering applications.

Variations of Heat Transfer Coefficient along the length:

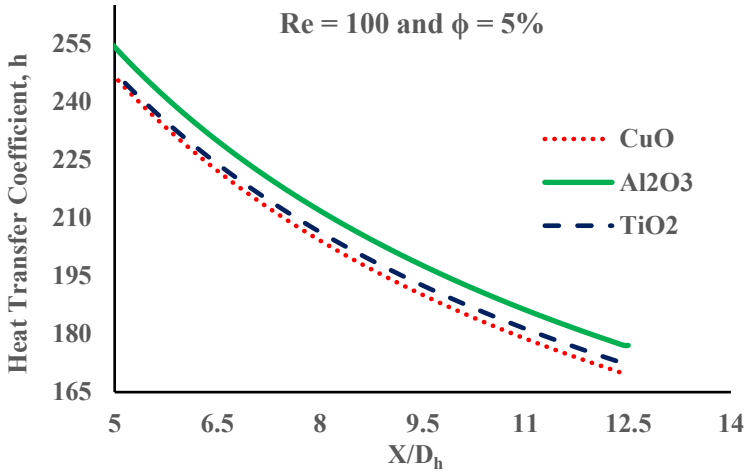

Fig. 6(a): Variations of Heat Transfer Coefficient of different nanofluids at ϕ = 5% and Re = 100

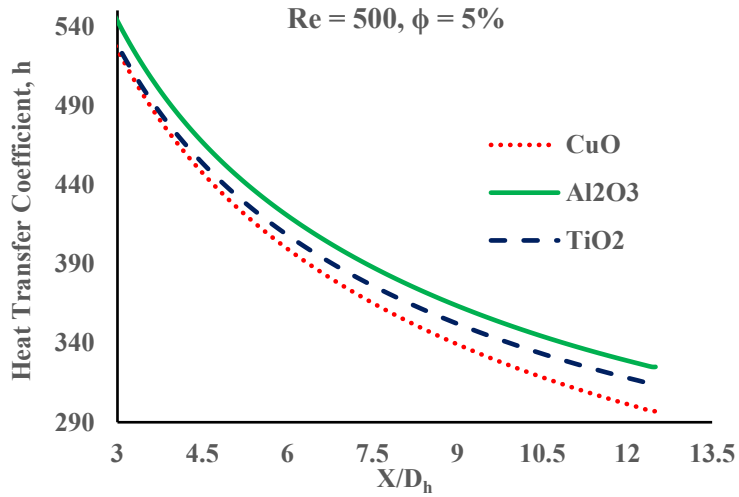

Fig. 6(b): Variations of Heat Transfer Coefficient of different nanofluids at ϕ = 5% and Re = 500

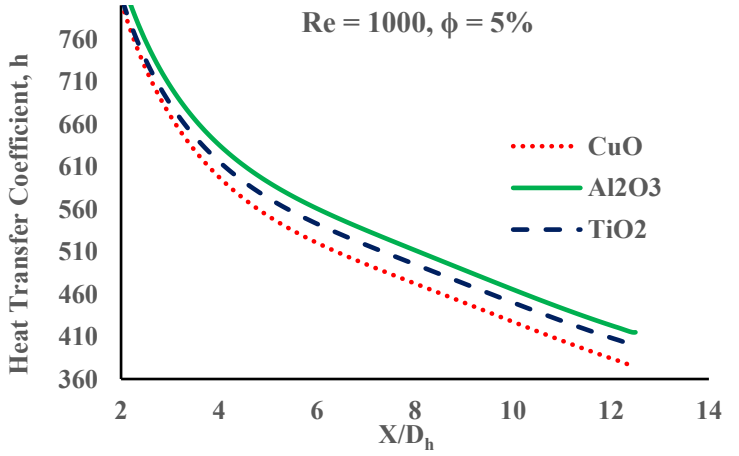

Fig. 6(c): Variations of Heat Transfer Coefficient of different nanofluids at ϕ = 5% and Re = 1000

Figures 6(a)–6(c) present the variation of the heat transfer coefficient (h) with dimensionless axial distance (X/D_h) for Al_2O_3–water, CuO–water, and TiO_2–water nanofluids at a particle concentration of ϕ = 5% under Reynolds numbers of 100, 500, and 1000. At Re = 100, the heat transfer coefficient decreases gradually along the duct, which corresponds to the thickening of the thermal boundary layer. In this regime, Al_2O_3–water achieves the

International Journal of Environmental Sciences
ISSN: 2229-7359
Vol. 11 No. 24s, 2025
https://theaspd.com/index.php

highest values, TiO_2–water lies in the middle, and CuO–water shows the lowest performance. The superiority of Al_2O_3–water is attributed to its higher effective thermal conductivity and better energy transport characteristics. At Re = 500, stronger convection enhances heat transfer, leading to larger values of h compared to Re = 100. The order of performance remains unchanged, with Al_2O_3–water maintaining dominance. TiO_2–water exhibits moderate improvement, while CuO–water continues to be less effective. The flatter slope of the profiles suggests quicker attainment of fully developed conditions. At Re = 1000, the heat transfer coefficient reaches its maximum, confirming the strong influence of forced convection. Overall, Al_2O_3–water provides the most effective balance between enhanced heat transfer and manageable flow resistance.

Variations of Heat Transfer Coefficient with respect to Re:

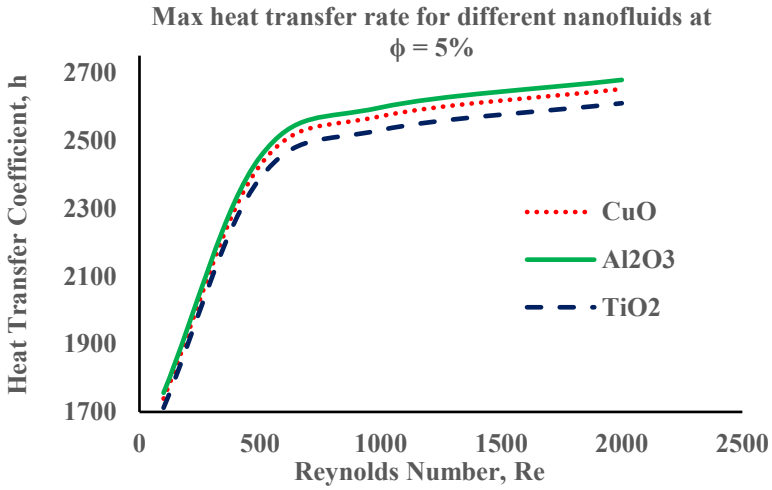

Fig. 7(a): Variations of Heat Transfer Coefficient with Reynolds number of different nanofluids at ϕ = 5%

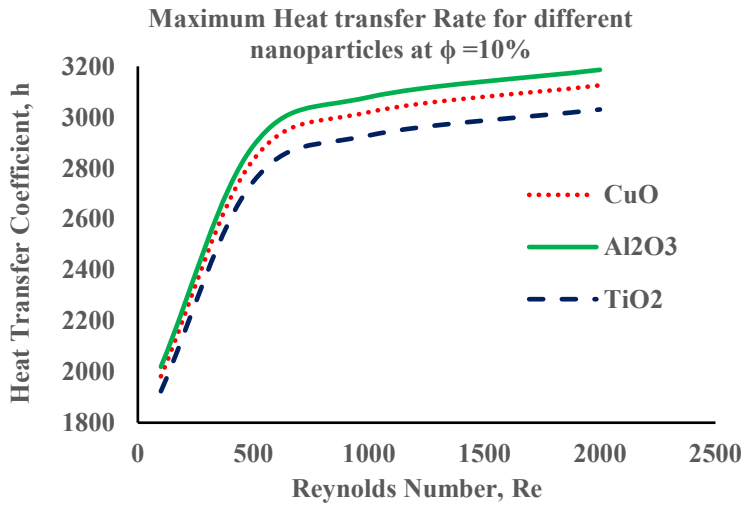

Fig. 7(b): Variations of Heat Transfer Coefficient with Reynolds number of different nanofluids at ϕ = 10%

Figures 7(a) and 7(b) depict the maximum heat transfer coefficient (h) of CuO–water, Al_2O_3–water, and TiO_2–water nanofluids as a function of Reynolds number (Re) at particle loadings of 5% and 10%. The results indicate that Al_2O_3–water consistently achieves the highest heat transfer coefficient, followed by CuO–water, while TiO_2–water provides the lowest enhancement. The superior performance of Al_2O_3 is mainly linked to its higher thermal conductivity and better dispersion stability, which promote efficient thermal transport.A comparison between concentrations shows that increasing nanoparticle volume fraction from 5% to 10%significantly improves the heat transfer coefficient for all nanofluids, underlining the influence of particle loadingon convective heat transfer enhancement. Moreover, the effect of Reynolds number is evident, with higher flowrates leading to substantial increases in h due to stronger convective mechanisms. At elevated Reynolds numbers,the curves tend to plateau, suggesting that once forced convection dominates, additional improvements becomelimited. Overall, Al_2O_3–water at higher concentrations emerges as the most effective nanofluid for maximizingthermal performance.

International Journal of Environmental Sciences
ISSN: 2229-7359
Vol. 11 No. 24s, 2025
https://theaspd.com/index.php

Variations of Nusselt Number with ϕ and Re:

Similarly, the increase in Nusselt number of the nanofluid has been achieved with the increase of nanoparticle percentage and Reynolds number as shown in fig. 8(a) to 8(c).

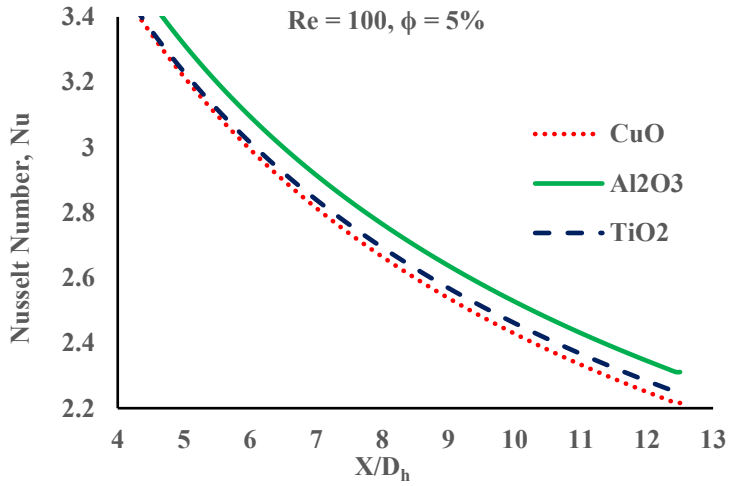

Fig. 8(a): Variations of Nusselt number of different nanofluids at ϕ = 5% and Re = 100

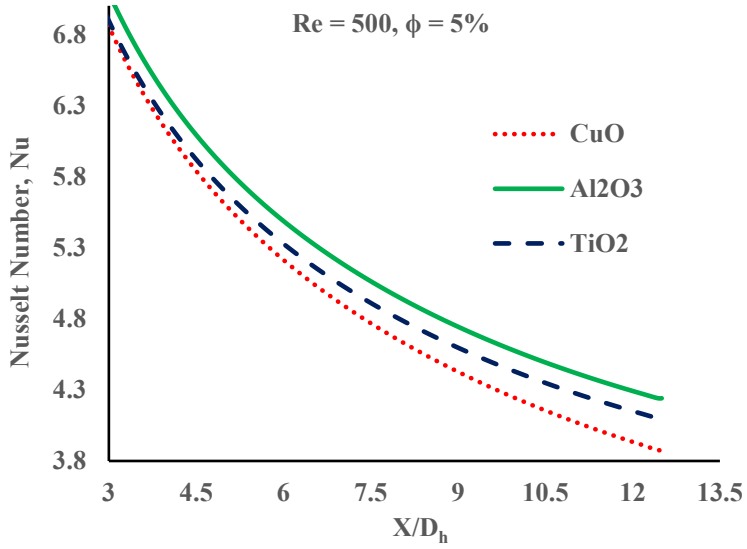

Fig. 8(b): Variations of Nusselt number of different nanofluids at ϕ = 5% and Re = 500

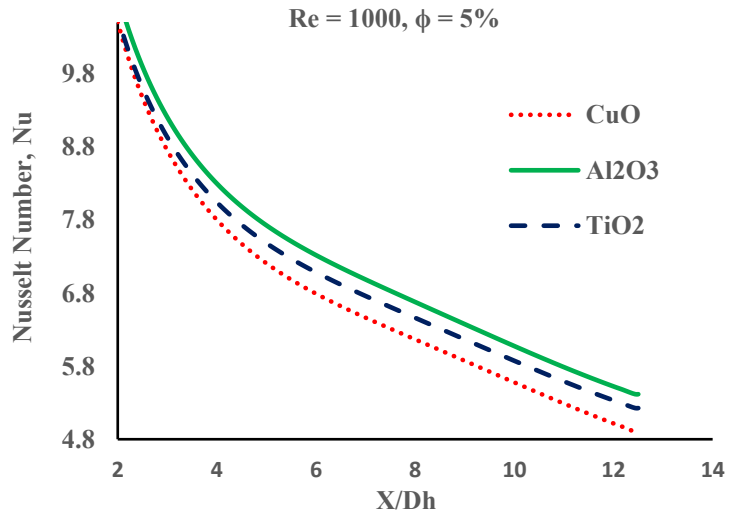

Fig. 8(c): Variations of Nusselt number of different nanofluids at ϕ = 5% and Re = 1000

Figures 8(a)–8(c) present the variation of the local Nusselt number (Nu) with dimensionless axial distance (X/Dh) for Reynolds numbers of 100, 500, and 1000 at a constant nanoparticle concentration of 5%. The study compares

CuO–water, Al_2O_3–water, and TiO_2–water nanofluids to evaluate the effect of particle type on convective heat transfer. In each case, Nu decreases progressively along the duct, reflecting the shift from the entrance region to the thermally developed regime. Elevated Nu values near the inlet correspond to the initial growth of the thermal boundary layer, while further downstream, its thickening reduces heat transfer, causing Nu to approach a stable asymptote in line with classical convection theory.

Across all Reynolds numbers, Al_2O_3–water consistently yields the highest Nusselt numbers, TiO_2–water provides intermediate performance, and CuO–water results in the lowest enhancement. The superior results of Al_2O_3–water is linked to its higher thermal conductivity and better stability, which facilitate more effective thermal transport. In contrast, CuO–water demonstrates limited augmentation despite its higher density. These results emphasize that both Reynolds number and nanoparticle type govern thermal behaviour. Increasing Re strengthens convective transport, while Al_2O_3–water proves to be the most efficient option for applications such as compact heat exchangers and cooling systems.

Comparision of Nusselt Number:

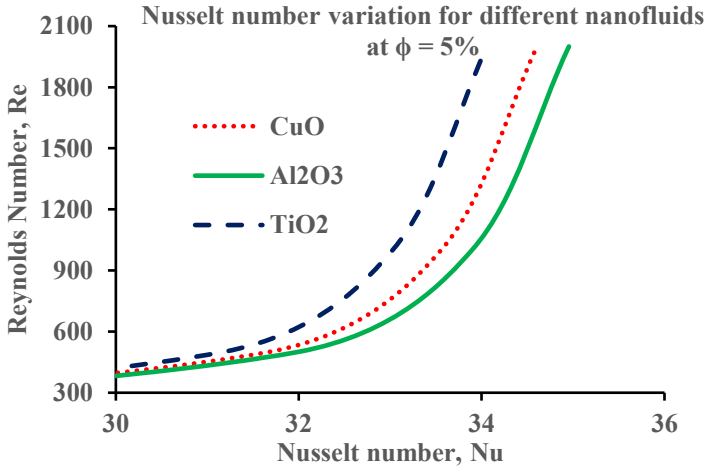

Fig. 9(a): Variations of Nusselt number with Reynolds number of different nanofluids at ϕ = 5%

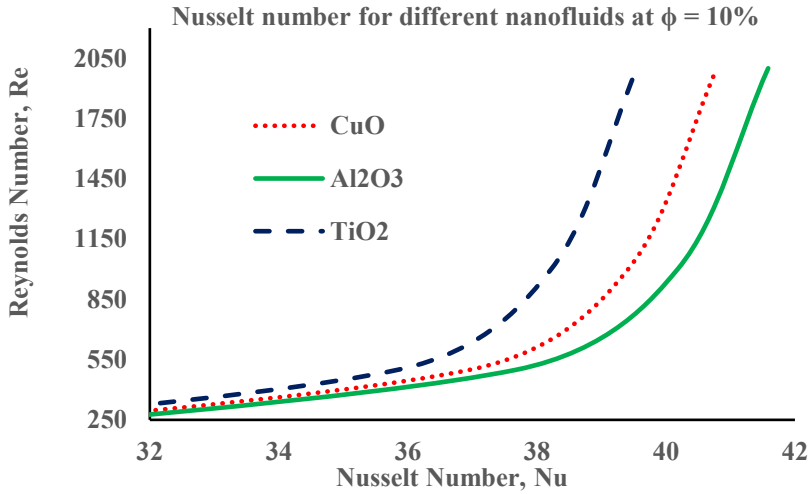

Fig. 9(b): Variations of Nusselt number with Reynolds number of different nanofluids at ϕ = 10%

Figures 9(a) and 9(b) depict the variation of the Nusselt number (Nu) with Reynolds number (Re) for CuO–water, Al_2O_3–water, and TiO_2–water nanofluids at particle loadings of ϕ = 5% and ϕ = 10%. The results demonstrate the influence of both nanoparticle type and concentration on convective heat transfer. At ϕ = 5% [Figure 9(a)], Al_2O_3–water consistently records the highest Nu values at a given Re, confirming its superior thermal performance over CuO– and TiO_2–based nanofluids. Al_2O_3–water also shows enhanced heat transfer even at relatively lower Re, highlighting its ability to promote stronger boundary layer disruption and mixing under laminar-to-transitional conditions.

When the concentration is increased to ϕ = 10% [Figure 9(b)], the same trend persists, with Al_2O_3–water maintaining its dominance, CuO–water providing moderate improvement, and TiO_2–water offering the least enhancement. The rise in Nu across all nanofluids at higher particle loading reflects the positive role of increased

thermal conductivity and energy transport due to greater nanoparticle presence. Overall, these results confirm that both nanoparticle material and concentration are decisive factors for heat transfer improvement. Al_2O_3–water emerges as the most efficient nanofluid, making it well-suited for advanced cooling and thermal management applications.

Variations of Heat Transfer Coefficient and Nusselt Number with Nanolayer Thickness:

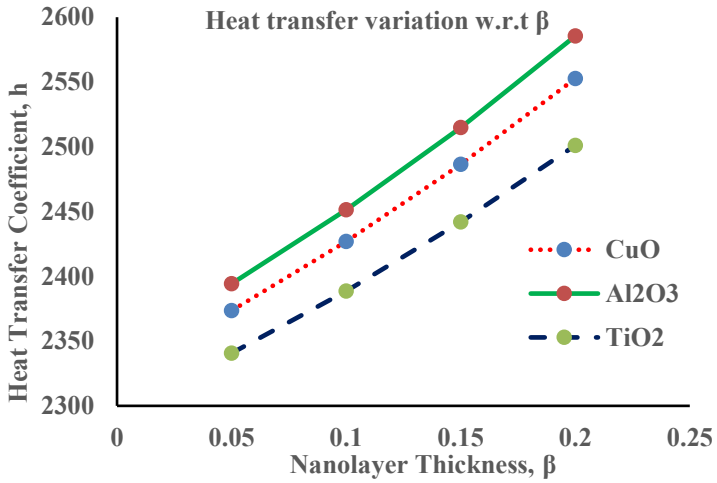

Fig. 10(a): Variations of Heat Transfer Coefficient with Nanolayer Thickness of different nanofluids at ϕ = 5%

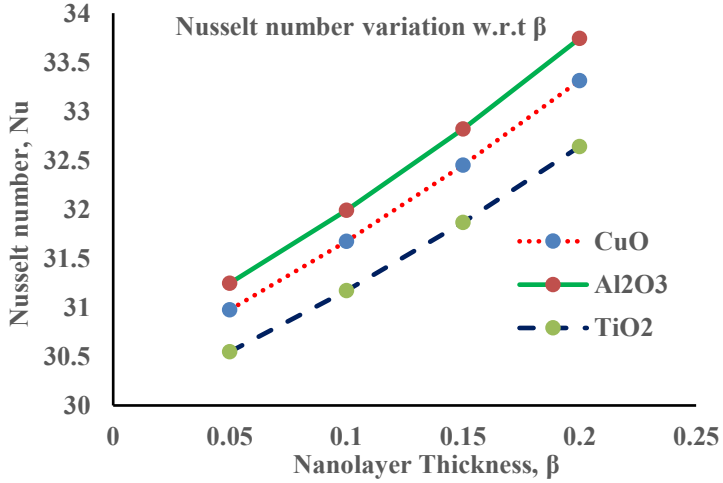

Fig. 10(b): Variations of Nusselt Number with Nanolayer Thickness of different nanofluids at ϕ = 5%

Figures 10(a) and 10(b) show the impact of nanolayer thickness (β) on the heat transfer coefficient (h) and the Nusselt number (Nu) for CuO–water, Al_2O_3–water, and TiO_2–water nanofluids. From Figure 10(a), it is evident that h increases almost linearly with β for all nanofluids. Al_2O_3–water records the highest enhancement, followed by CuO–water and then TiO_2–water. At β = 0.20, the heat transfer coefficient of Al_2O_3–water reaches nearly 2575 W/m²K, which is about 3–5% higher than CuO–water and 6–7% greater than TiO_2–water. This superior performance is attributed to stronger interfacial thermal interactions between Al_2O_3 nanoparticles and the base fluid, which promote more effective energy exchange.

Figure 10(b) depicts the variation of Nu with nanolayer thickness, showing a similar upward trend. Al_2O_3–water again achieves the highest values, with Nu ≈ 33.8 at β = 0.20, compared to 33.3 for CuO–water and 32.7 for TiO_2–water. The consistent order of performance across both parameters highlights the significant role of nanolayer effects in governing convective heat transfer. In summary, increasing nanolayer thickness enhances thermal performance for all nanofluids, with Al_2O_3–water proving to be the most efficient due to its superior conductivity and strong fluid compatibility.

CONCLUSIONS:

A three-dimensional numerical analysis was conducted to investigate the conjugate heat transfer performance of nanofluid–water mixtures flowing through a rectangular duct under steady laminar conditions. The study focused on Al_2O_3–water, CuO–water, and TiO_2–water nanofluids, examining the effects of Reynolds number and

nanoparticle concentration on both hydrodynamic and thermal characteristics. The findings show that incorporating nanoparticles markedly improves convective heat transfer compared with the base fluid, as indicated by higher Nusselt numbers and heat transfer coefficients. Increasing Reynolds number further enhances transport, reflecting the combined influence of flow inertia and nanoparticle dispersion.

Among the studied suspensions, Al_2O_3–water consistently demonstrates the most favourable trade-off between thermal enhancement and frictional resistance, while CuO–water and TiO_2–water provide moderate gains. Validation of velocity profiles with published results confirms the accuracy of the model. These outcomes highlight the importance of careful nanofluid and flow parameter selection to achieve efficient thermal management with limited pumping penalties.

Future work may extend this investigation to consider non-Newtonian effects, two-phase models, offering further insight into practical implementation scenarios.

REFERENCES:

[1] Choi., and Eastman., (1995) Enhancing Thermal Conductivity of Fluids with Nanoparticles. Energy Technology Division and Materials Science Division; Argonne National Laboratory, Argonne.
[2] Xuan. Y., and Li, Q. (2000) Heat transfer enhancement of nanofluids. International Journal of Heat and Fluid Flow. Vol. 21, pp. 58-64.
[3] Akbarinia, A., and Behzadmehr, A., (2007) Numerical study of laminar mixed convection of a nanofluid in horizontal curved tubes. Applied Thermal Engineering. Vol. 27, pp. 1327-1337.
[4] Wang, X., and Mujumdar, A. S., (2008) Heat transfer characteristics of nanofluids: A review. International Journal of Thermal Sciences. Vol. 47(7), pp. 1053–1063.
[5] Kakaç, S., and Pramuanjaroenkij, A., (2009). Review of convective heat transfer of nanofluids. Energy Conversion and Management. Vol. 50(7), pp. 1618–1628.
[6] Malvandi, A., & Galanis, N., (2012). A review of the effects of nanoparticles on the heat transfer characteristics of nanofluids. Nanoscale Research Letters. Vol.7(1), pp. 1–13.
[7] Vanaki, S, M., Ganesan, P., and Mohammed, H, A., (2015) Numerical study of convective heat transfer of nanofluids: A review. Renewable and Sustainable Energy Reviews. Vol. 54, pp.1212–1239.
[8] Patankar S.V., (1980) Numerical Heat Transfer and Fluid Flow. Hemisphere Publishing Corporation. New York, USA.
[9] Kirez, O., Yazicioglu, A., and Kakac, S., (2013) Numerical analysis of convective heat transfer of nanofluids for laminar flow in a circular tube. International Mechanical Engineering Congress and Exposition. pp. 471-478.
[10] Heris, SZ., Noie, SH., Talaii, NE., and Sargolzaei, J., (2011) Numerical investigation of Al_2O_3/water nanofluid laminar convective heat transfer through triangular ducts. Nanoscale Research Letters. Vol. 6(179), pp. 1-10.
[11] Bouhalleb, M., Abbassi, H., (2016) Numerical Investigation of Heat Transfer by CuO–Water Nanofluid in Rectangular Enclosures. Heat Transfer Engineering. Vol. 37(1) pp. 13–23.
[12] Vasefi, I., and Alizadeh, M. A., (2013) Numerical Investigation of Cuo-Water Nanofluid in Different Geometries by Two-Phase Euler-Lagrange Method. World Applied Sciences Journal. Vol. 26(10), pp. 1323-1329.
[13] Elyasi, P., and Ziaei-Rad, M., (2013) Investigation of Laminar Pulsating Nanofluid Flow and Heat Transfer in a Rectangular Channel. Journal of Nanostructures, Vol. 3, pp. 289-301.
[14] Sundar, L. S., and Suresh, S., (2017). Conjugate heat transfer analysis of nanofluid in microchannel. International Journal of Thermal Sciences. Vol. 118, pp. 39–49.
[15] Jafari, R., and Aminossadati, S. M., (2011). Conjugate heat transfer analysis of nanofluid flow in a pipe with circular cross-section. International Journal of Heat and Mass Transfer. Vol. 54(11), pp. 2683–2692.
[16] Rabby, Md. I.I., Siti Ujila Masuri, S.U., Lingeswaran Kaniappan, L., Loulou, T. and Islam, A K M. S., (2019) Effect of Water Based Nanofluids on Laminar Convective Heat Transfer in Developing Region of Rectangular Channel. CFD Letters. Vol.11, No.12, pp. 74-87.
[17] Kashani A, Jalali-Vahid, D., and Hussainpour, S., (2013) Numerical Study of Laminar Forced Convection of Water/Al_2O_3 Nanofluid in an Annulus with Constant all Temperature. IIUM Engineering Journal. Vol. 14(1), pp. 77-92.
[18] Irmawati, N., and Mohammed, HA., (2015) Mixed Convective Heat Transfer in Water-Based Al_2O_3 Nano fluid in Horizontal Rectangular Duct. International Journal of Mechanical, Aerospace, Industrial. Mechatronic and Manufacturing Engineering.Vol. 8(12), pp. 2083-2086.
[19] Boukerma, K., and Kadja, M., (2017) Convective Heat Transfer of Al_2O_3 and CuO Nanofluids Using Various Mixtures of Water - Ethylene Glycol as Base Fluids. Engineering, Technology & Applied Science Research. Vol. 7(2), pp. 1496-1503.
[20] Khudheyer, F Ahmed and Hameed., and A, Raghad., (2018) Numerical Investigation of Forced Convection Heat Transfer on a Circular Finned tube with AL_2O_3-Water Nano Fluid. International Journal of Scientific Research and Management (IJSRM). Vol. 6, pp. 26-34.
[21] Murshed, S.M.S., Leong, K.C., Yang, C. and Nguyen, N.T., (2008) Convective Heat Transfer Characteristics of Aqueous TiO_2 Nanofluid under Laminar Flow Conditions. International Journal of Nanoscience. Vol. 7, No. 6, pp. 325–331.
[22] Bianco, V., Marchitto, A., Scarpa, F., and Tagliafico, LA., (2019) Numerical investigation on the forced laminar convection heat transfer of Al_2O_3-water nanofluid within a three-dimensional asymmetric heated channel. International Journal of Numerical Methods for Heat & Fluid Flow. Vol. 29(3), pp. 1132-1152.
[23] Barad, V.S., Makwana, N.M., (2014) Numerical Investigation of Single-Phase Fluid Flow and Heat Transfer in Rectangular Micro Channel Using Nanofluids as A Cooling Liquid. Int. Journal of Engineering Research and Applications. Vol. 4, pp.133-137.
[24] Omid, M., Ali, K., Clement, K., Al-Nimr, MA., Pop, I., Sahin, AZ., and Somchi, W., (2013) A Review of Entropy Generation in Nanofluid Flow. International Journal of Heat and Mass Transfer. Vol. 65, pp. 514-532.